Korean J. Chem. Eng., 33(10), 2802-2807 (2016)
DOI: 10.1007/s11814-016-0238-8
pISSN: 0256-1115
eISSN: 1975-7220

RAPID COMMUNICATION

Photocatalytic degradation of bromophenol blue in aqueous medium using chitosan conjugated magnetic nanoparticles

Hamayun Khan*,†, Abdul Kabir Khalil*,, Adnan Khan**, Khalid Saeed***, and Nauman Ali****

*Department of Chemistry, Islamia College University, Peshawar 25120, Pakistan
**Institute of Chemical Sciences, University of Peshawar, Peshawar 25120, Pakistan
***Department of Chemistry, University of Malakand, Chakdara, Dir(L), Pakistan
(*Received 24 April 2016 • accepted 19 August 2016*)

Abstract−Three different chitosan conjugated magnetic nanoparticles (CCMN) of Co, Ni and Fe were prepared using co-precipitation method. The prepared CCMN were characterized by scanning electron microscopy (SEM), X-ray diffraction (XRD) and Fourier transform infra-red (FT-IR) spectroscopic techniques. The SEM results showed a smooth surface morphology with almost uniform particle size and irregular shape structure for all CCMN. The XRD study revealed the crystalline structure in case of Co-CCMN and Ni-CCMN, while amorphous nature of Fe-CCMN was observed. The particle size of the prepared CCMN was found to be <95 nm, as confirmed from SEM and XRD analyses. Similarly, FT-IR analysis showed the incorporation and conjugation of Co, Ni and Fe magnetic nanoparticles into the chitosan polymer matrix. The point of zero charge (PZC) was found to be 7.41 for Co-CCMN and Ni-CCMN and 7.70 for Fe-CCMN. The photocatalytic activity of the prepared CCMN was investigated under UV light irradiation (254 nm and 15 W) in the aqueous medium using bromophenol blue (BPB). The photocatalytic process was monitored by UV-visible spectrophotometer for different irradiation times (0 to 10 h). The results showed that all the prepared CCMN displayed good to excellent photocatalytic property where the highest degradation was exhibited by Fe-CCMN (94.5%), followed by Co-CCMN (85.1%) and Ni-CCMN (83.0%). The prepared catalysts were recycled and reused, maintaining good photocatalytic activity for four consecutive batches.

Keywords: Photocatalysis, Chitosan, Magnetic Nanoparticles, Bromophenol Blue

INTRODUCTION

Various industries, such as textile, paper, plastic, leather, food, pharmaceutical, and cosmetic, use dyes and pigments in their products. The effluents coming from these industries are highly colored, which pose a threat to the environment as well as living organisms even at low concentration. The treatment of such wastewater is a challenging task as most of the dyes are non-degradable and persist for a long time [1-7]. There are number of methods and techniques are available for the treatment of colored water and wastewater. The common include precipitation, flotation, flocculation, coagulation, ozonization, reverse osmosis, ultrafiltration and adsorption [1-5]. In recent times, widespread investigation has focused on new techniques, such as ozonation, electrochemical, Fenton and UV/H_2O_2 treatments; ultrasonic, radiolytic, bio-, photo- and photocatalytic degradations [8-20].

Nanotechnology is a modern robust technique through which the material produced has smaller particle size (<100 nm), large surface area and more efficacious. These smart nanomaterials find numerous applications in almost every field of science. Magnetic nanoparticles, particularly the spinal class, stand the most interesting magnetic oxides broadly used due to their exciting magnetic, electrical, optical and photocatalytic and drug carrier properties [21,22]. In the realm of nanoparticles, the stuff of magnetic nanoparticles intensely rests on the particle size. The various methods used for the preparation of magnetic nanoparticles include sol-gel, forced hydrolysis in a polyol medium, oil-in-water micelles, inverse micelles and thermal decomposition [23]. However, most of these protocols are tedious and expensive. Preparation of magnetic nanoparticles via co-precipitation method provides the best alternative for the cost-effective production of ultra-fine nanoparticles with high yield [22-24].

Keeping in view the importance of magnetic nanoparticles and their applications, we undertook the present study. Three different magnetic nanoparticles of Co, Ni and Fe were conjugated with chitosan using co-precipitation method. The prepared CCMN were characterized and applied for the photocatalytic degradation of industrially important dye, i.e., bromophenol blue (BPB). The removal and degradation of BPB have been reported in the literature [18,23-37]. However, to the best of our knowledge, this is the first report on the photocatalytic degradation of BPB in the aqueous medium using CCMN.

MATERIALS AND METHODS

1. Materials

Analytical grade chemicals were used. Chitosan powder, CH_3COOH, $FeSO_4{\cdot}7H_2O$ and $FeCl_3{\cdot}6H_2O$ were purchased from Merck (Germany); urea, NH_4OH, $NiSO_4{\cdot}7H_2O$, $CoSO_4{\cdot}7H_2O$ were purchased from Sigma-Aldrich (USA) and bromophenol blue (BPB) was

†To whom correspondence should be addressed.
E-mail: hamayun84@yahoo.com

obtained from EYER® Chemical Reagent (China). Deionized double distilled water (DDDW) was used throughout the experimental work.

2. Preparation of Chitosan Solution

0.5% w/v solution of chitosan was prepared by dissolving the required amount of chitosan powder in 1% v/v aqueous acetic acid solution.

3. Preparation of $FeCl_3$ Solution of Co, Ni and Fe

The $FeCl_3$ solution of Co, Ni and Fe was prepared separately using $FeCl_3$ and $CoSO_4 \cdot 7H_2O$, $FeCl_3$ and $NiSO_4 \cdot 7H_2O$ and $FeCl_3$ and $FeCl_3 \cdot 6H_2O$ in equimolar ratio using DDDW.

4. Preparation of Chitosan Conjugated Magnetic Nanoparticles

Chitosan conjugated magnetic nanoparticles (CCMN) of Co, Ni and Fe were prepared separately by co-precipitation method. Briefly, $FeCl_3$ solutions of Co, Ni and Fe were mixed vigorously with chitosan solution in 1 : 2 stoichiometric ratio, separately. To this mixture, 15 g urea was added, followed by the dropwise addition of NH_4OH solution (3.5 M) until pH 11 was attained. After the co-precipitation, the products obtained were washed thoroughly with DDDW until neutral pH. The precipitated products were dark black in the case of Co and Fe while brown for Ni-CCMN. The prepared CCMN was heated at 80 °C for 30 min in an oven (LDO-030E, Daihan Lab Tech Co., Ltd., South Korea) and stored in air-tight vessels till further use.

5. Characterizations

The prepared CCMN were characterized using scanning electron microscopy (SEM), X-ray diffraction (XRD) and Fourier transform infra-red (FT-IR) spectroscopy. For SEM, a JEOL JSM-5910 (Japan) scanning electron microscope was used. The samples were gold-coated and the SEM images were obtained. The powder XRD analysis was performed using a JEOL JDX-9C-XRD (Japan) spectrometer in the 2θ range from 10 to 50° with Cu Kα radiation at room temperature. The count time was 0.5 sec while the tube voltage and current was 40 kV and 30 mA, respectively. For FT-IR data, the CCMN were directly analyzed using ATR system (Thermo Electron Corporation, USA) equipped with Thermo Scientific Nicolet 6700 FT-IR spectrometer with wavenumber varied from 4,000 to 400 cm^{-1}. The PZC was determined using the reported method [18,27].

6. Photocatalytic Degradation of BPB

The photocatalytic properties of CCMN were studied by using an aqueous solution of BPB. For this purpose, CCMN (0.1 g) was mixed with 10 mL of BPB solution (30 mg/L) in a cleansed vial, placed on a magnetic stirrer in the dark for 30 min in order to allow the adsorption-desorption equilibrium to be reached. The mixture was then irradiated under UV light (low pressure Hg vapor lamp, emitting predominantly at 254 nm and 15 W) for different time of intervals (0 to 10 h) at a neutral pH. After a definite irradiation time, CCMN was separated by centrifugation, the absorbance and concentration of BPB solution was determined using a double beam UV-visible spectrophotometer (UV-1602, Biotechnology Medical Services, BMS, USA). The samples were periodically removed for the determination of BPB, both during the dark adsorption stage as well as during photocatalytic degradation. The percent degradation of BPB was calculated with the following equations [12,13]:

$$\% \text{ Degradation: } \frac{Ao - A}{Ao} \times 100$$

$$\% \text{ Degradation: } \frac{Co - C}{Co} \times 100$$

where Ao and A represent the absorbance of BPB solution before and after UV light irradiation, respectively. Similarly, Co and C are the concentration (mg/L) of BPB solution before and after UV light irradiation, respectively. The λ_{max} of BPB solution was found to be 590 nm. The catalysts were recycled and reused for four consecutive batches using the above conditions [18,20].

RESULTS AND DISCUSSION

1. Characterizations of the Prepared CCMN

The prepared CCMN were characterized by using SEM, XRD and FT-IR spectroscopic techniques. The morphology and surface topography of the prepared CCMN were studied with SEM (Fig. 1). As can be seen from the results, all the prepared CCMN have smooth surfaces with almost homogenized particle size and shape. The structure of CCMN was slightly irregular as confirmed from SEM images. The particle size was 89±6, 82±4 and 85±5 nm for Co-CCMN, Ni-CNMN and Fe-CCMN, respectively (Fig. 1).

The lattice structure of the prepared CCMN was investigated by using XRD analyses (Fig. 2). The analysis was done to determine the effect of magnetic nanoparticles on the crystallinity of precursor chitosan. The pure chitosan showed a diffraction XRD pattern that presents poor crystallinity, as can be seen through the characteristic broad peak (Fig. 2(b)). The results revealed the crystal pat-

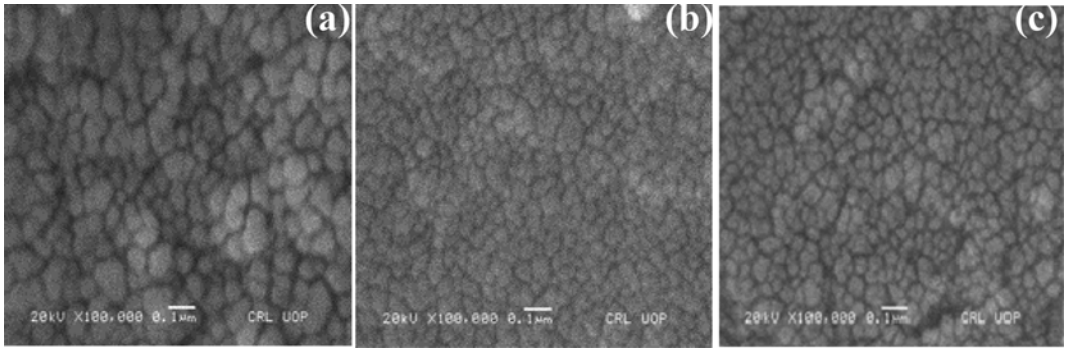

Fig. 1. SEM images of CCMN, (a) Co-CCMN, (b) Ni-CCMN and (c) Fe-CCMN.

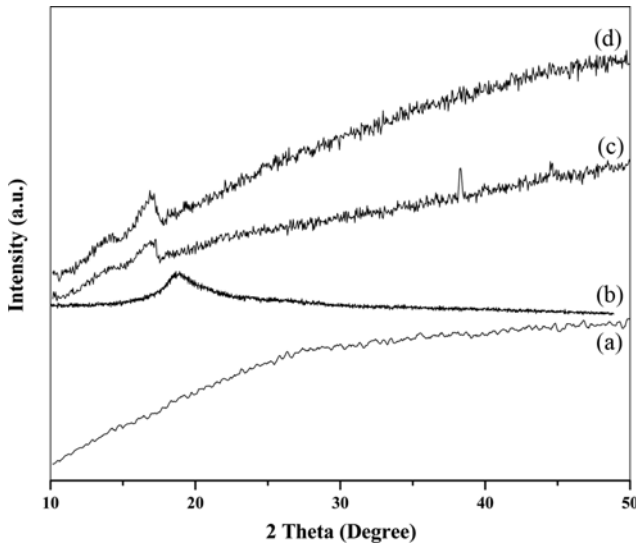

Fig. 2. XRD patterns of CCMN, (a) Fe-CCMN, (b) Chitosan, (c) Ni-CCMN and (d) Co-CCMN.

terns of Co-CCMN and Ni-CCMN while Fe-CCMN was found to be amorphous. The crystallinity pattern was in order of Co-CMMN≥Ni-CMMN>Fe-CMMN. From the XRD data, the particle size of CCMN was determined by Debye-Scherrer equation as given below [3,17,24,30];

$$d = \frac{0.9\lambda}{\beta\cos\theta}$$

where d is the average crystal size (nm), λ 1.5406 Å (CuKα radiation as the X-ray source) and β represents the full width at half-maximum for a diffraction peak. The average particle size was 88.5±4.6 and 89.1±4.1 nm, respectively, for Co-CCMN and Ni-CCMN, while Fe-CCMN was amorphous. These results are in accordance with the SEM data. In a previous study, the particle sizes determined by SEM were found to differerent significantly from the particle sizes calculated using XRD data [17]. The smaller particle sizes with narrow particle size distribution are reported herein.

The functional groups of the prepared CCMN were determined using FT-IR spectroscopic technique. The FT-IR spectra of CCMN were compared with the spectrum of pristine chitosan as shown in Fig. 3. The original chitosan showed an intense and large characteristic at 3,400 cm^{-1} due to stretching vibration of the hydroxyl group of citizen structure. The bands at 2,925 and 2,875 cm^{-1} are due to symmetric and asymmetric stretching vibration of C-H bond of chitosan. The band found at 1,657 cm^{-1} is associated with amide group. Similarly, an intense band at 1,076 cm^{-1} is due to C-O-C stretching vibration of the glucosidic ring, and the peak at 1,4-glycosidic bond [38-40]. As compared to the FT-IR spectrum of the pristine chitosan, the appearance of some extra peaks (particularly at 664 and 558 cm^{-1} due to magnetic nanoparticles) and slight shift in the position of other peaks may be due to the incorporation and conjugation of Co, Ni and Fe magnetic nanoparticles into the chitosan polymer matrix as $CoFe_2O_4$, $NiFe_2O_4$ and Fe_3O_4. Noticeable changes have been observed in the spectra of CCMN. The appearance of the band at 558 cm^{-1} is attributed to metal-oxygen bond as shown in Fig. 3. Also, the peak of precursor chitosan to at 1,076 cm^{-1} is shifted to 664 cm^{-1} in the spectra of CCMN (Chitosan-$CoFe_2O_4$, Chitosan-$NiFe_2O_4$ and Chitosan-Fe_3O_4), demonstrating a successful synthesis of the material. This also confirms the applicability of the prepared CCMN for decontamination of various pollutants [5,38-40].

The PZC of the prepared CCMN was determined and found to be 7.41 for Co-CCMN and Ni-CCMN and 7.70 for Fe-CCMN (Fig. 4). This means that the surface of the prepared catalysts is positively and negatively charged when the pH values are below and above the PZC, respectively. BPB is an ionic dye with anionic nature in the aqueous medium. In the present study, all the degradation experiments were performed in aqueous medium at a neutral pH. It is therefore, deduced that there may be little or no interaction of BPB with CCMN under the studied conditions. In all the experiments, the reaction assembly (an aqueous solution of BPB and CCMN) was kept in the dark for 30 min to reach adsorption-

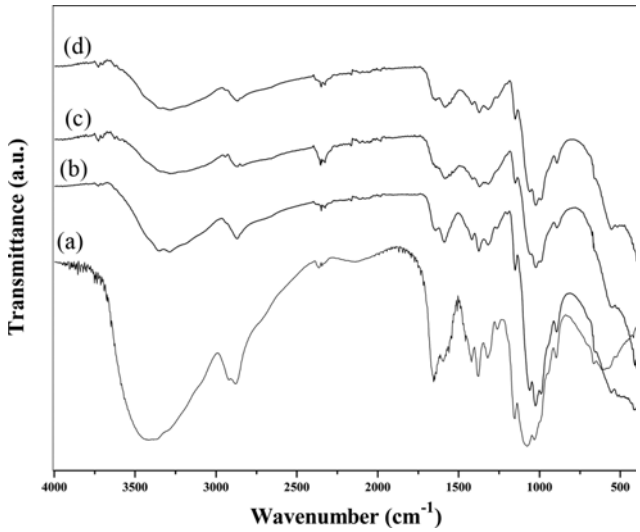

Fig. 3. FT-IR spectra of CCMN, (a) Chitosan, (b) Fe-CCMN, (c) Co-CCMN and (d) Ni-CCMN.

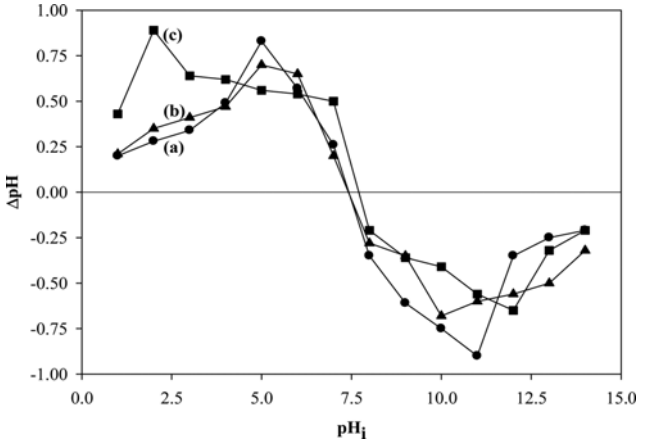

Fig. 4. PZC of the prepared CCMN, (a) Co-CCMN, (b) Ni-CCMN and (c) Fe-CCMN.

desorption equilibrium, if any, and then irradiated under UV-light; afterwards, the photocatalytic degradation process was monitored. The results of the original BPB solution and after 30 min stirring in the dark were the same (data not shown). This shows that BPB is degraded photocatalytically under UV-irradiation in the aqueous medium using CCMN. Similar results were also reported for the photocatalytic degradation of methylene blue in the aqueous solution using functionalized carbon nanotubes supported TiO_2 [12].

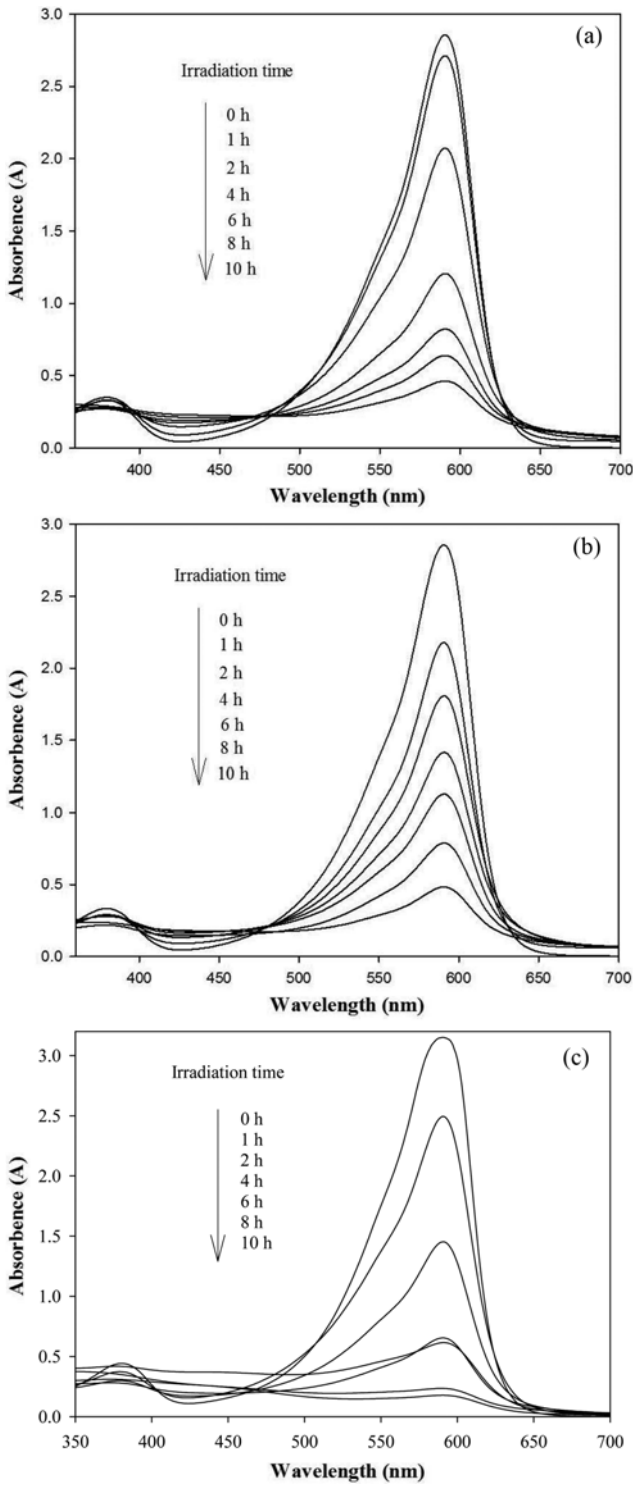

Fig. 5. UV-visible absorbance spectra of the photocatalytic degradation of BPB in aqueous medium using CCMN, (a) Co-CCMN, (b) Ni-CCMN and (c) Fe-CCMN.

2. Photocatalytic Degradation of BPB

The photocatalytic activity of the prepared CCMN was investigated under UV light irradiation in the aqueous medium using BPB as a model dye. Fig. 5 shows the UV-visible absorbance spectra of BPB in the aqueous medium before and after irradiation for time intervals of 0 to 10 h at a neutral pH. The results showed that with the increase of irradiation time (from 0 to 10 h), there was a continuous decrease in the absorbance of BPB solution at λ_{max} of 590 nm. This indicates that the photocatalytic degradation of BPB is time dependent and increases with increase in irradiation time (Fig. 5 & 6). As can be seen from the results, all the prepared CCMN displayed good to excellent photocatalytic activity against BPB in the aqueous medium. The photocatalytic degradation of BPB was found to be higher in case of Fe-CCMN (94.5%), followed by Co-CCMN (85.1%) and Ni-CCMN (83.0%) after 10 h of irradiation (Fig. 6).

In a typical photocatalytic system, the photocatalyst surface is responsible for photo-chemical reaction or photo-induced chemical transformation. The basic mechanism of photocatalytic reaction is governed by the generation of electron-hole pair (e^-+h^+) into the photocatalyst followed by free radical formation and its transportation to destination, i.e., reaction with the target chemical species such as dyes [3,11-13,30]. In the present study, the photocatalytic degradation of BPB in the aqueous medium is due to CCMN which act as photocatalysts. Four possible mechanisms have been proposed for the photocatalytic degradation of BPB in the aqueous medium using CCMN. During photocatalysis, CCMN first photo-excited to produce conduction band electrons (e^-) and valence band holes (h^+) when irradiated with UV light. The h^+ react with H_2O or OH^- and result in the formation of OH radical. The OH radical act as a strong oxidizing agent which degrades BPB upon reaction as presented below [3,11-13,30].

$$CCMN+hv \rightarrow CCMN\ (e^-+h^+)$$

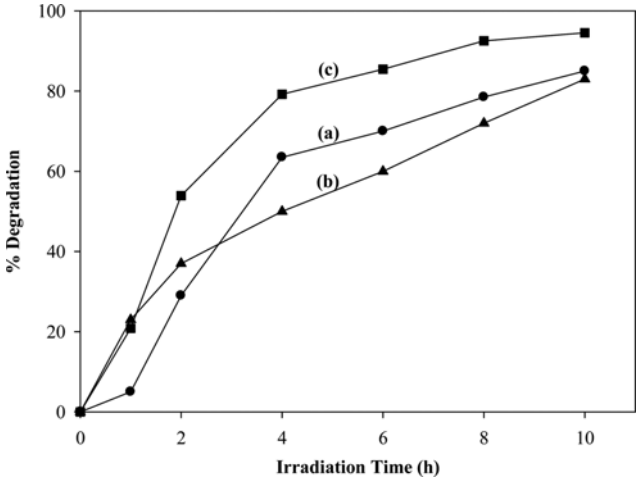

Fig. 6. Effect of irradiation time on the photocatalytic degradation of BPB in aqueous medium using CCMN, (a) Co-CCMN, (b) Ni-CCMN and (c) Fe-CCMN.

$CCMN\ (h^+)+H_2O \rightarrow CCMN+H^++OH^-$
$CCMN\ (h^+)+OH^- \rightarrow CCMN+OH^-$
$BPB+OH^- \rightarrow BPB\ Degradation$

The second possibility is the high oxidative potential of h^+, which directly degrades BPB as given below.

$CCMN\ (h^+)+BPB \rightarrow BPB^+ \rightarrow BPB\ Degradation$

The third option is that the e^- reduces dissolved oxygen and form superoxide anion radical ($O_2^{-\cdot}$) [11-13,26]. The $O_2^{-\cdot}$ is a also strong oxidizing agent, which reacts with BPB and degrade them.

$CCMN\ (e^-)+O_2 \rightarrow CCMN+O_2^{-\cdot}$
$BPB+O_2^{-\cdot} \rightarrow BPB\ Degradation$

Similarly, the e^- also reacts with dissolved oxygen; produce H_2O_2 and finally OH radical which then degrade BPB as highlighted below [11-20].

$CCMN\ (2e^-)+O_2+2H^+ \rightarrow CCMN+H_2O_2$
$CCMN\ (e^-)+H_2O_2 \rightarrow CCMN+OH^-+OH^-$
$BPB+OH^- \rightarrow BPB\ Degradation$

In a previous study, a possible mechanism for the photodegradation of BPB was suggested [18]. The prepared catalysts were recycled and reused for four consecutive batches, and the results showed that good photocatalytic activity was maintained by all the catalysts with an overall decrease of less than 6% as shown in Table 1. In a previous work, the photodegradation property of some catalysts decreased with an increase in the batches during the reusability [18]. The photocatalytic degradation of BPB was fitted with the first-order kinetics [$\ln (C/C_o)=-kt$], where C_o and C are the initial and final concentrations of BPB at time t, respectively, and k (min^{-1}) is the reaction rate constant, which was calculated from the slopes of the straight-line portion of the plots [19]. The values of k and rate of reaction were found to be 0.0047, 0.0034 and 0.0040 min^{-1} and 0.050, 0.051 and 0.054 ppm/min for Co-CCMN and Ni-CCMN while Fe-CCMN, respectively. Similar ranges of k values were also reported previously [19,31].

The heterogeneous photodecolorization of a mixture of methylene blue and BPB using CuO-nano-clinoptilolite was investigated previously and the results showed that the dyes were decolorized about 61 and 32%, respectively, under UV-irradiation [18]. Mashkour reported the adsorption assessed photodecolorization of BPB under UV-radiation using ZnO as a catalyst and almost 100% decolorization was achieved using 15 mg/L dye [29]. Photodegradation of BPB at low pH (<3) using fluorinated TiO_2 composites was investigated by Dlamini et al. They found that CNTs-TiO_2-F had the highest photocatalytic activity (98%) as compared to TiO_2 (85%) using 10 mg/L dye at 45±5 °C [30]. The photocatalytic decolorization of BPB in aqueous solution with different types of TiO_2 as photocatalysts in slurry form was carried out using UV-A light at 365 nm, and 70 to 90% of dye was removed using 10 mg/L dye [31]. The plasma-chemical and photocatalytic degradation of BPB was reported in the aqueous medium using TiO_2 as a catalyst with removal efficiencies ranged from 61.21 up to 82.05% [32]. The enzymatic decolorization of BPB was studied using native horseradish and citraconic anhydride-modified horseradish peroxidase with removal efficiency of about 96.1 to 97.8%, respectively [33]. In a previous study, oxidative decolorization and degradation of BPB with H_2O_2 catalyzed by Cu(II)-supported alumina and zirconia was reported, which showed that 60% of the dye carbon atoms are degraded and transformed to CO_2 [34]. The photocatalytic oxidation and degradation of BPB at low pH with potassium dichromate was reported using UV, solar irradiation, UV in combination with two diprotic acids (sulfuric and oxalic acids) and UV chromate/oxalate system. The results suggested that alone UV and solar exposure was the poor decolorizer of the dye, i.e., up to 10% [37]. The results obtained in the present study are more superior as compared to the reported literature discussed above.

Table 1. Recycling and reuse of CCMN

CCMN	No. of batches of recycling and reuse			
	1st	2nd	3rd	4th
	%Degradation			
Co-CCMN	84.9	83.6	82.7	81.1
Ni-CCMN	82.8	81.6	80.4	78.6
Fe-CCMN	94.1	92.9	91.2	89.1

CONCLUSION

Conjugated chitosan bimetallic magnetic nanoparticles with narrow particle size were successfully prepared and characterized. The photocatalytic potential of the prepared nanoparticles was explored using BPB as a model environmental pollutant. The admirable finding indicated that the prepared nanoparticles could be a suitable candidate for the treatment of colored water and industrial effluents.

REFERENCES

1. E. Forgacs, T. Cserhati and G. Oros, *Environ. Int.*, **30**, 953 (2004).
2. K. Singh and S. Arora, *Crit. Rev. Environ. Sci. Technol.*, **41**, 807 (2011).
3. M. Moradi, F. Ghanbari, M. Manshouri and K. A. Angali, *Korean J. Chem. Eng.*, **33**, 539 (2016).
4. T. Robinson, G. McMullan, R. Marchant and P. Nigam, *Bioresour. Technol.*, **77**, 247 (2001).
5. W. S. W. Ngah, L. C. Teong and M. A. K. M. Hanafiah, *Carbohydr. Polym.*, **83**, 1446 (2011).
6. H. Khan, S. Haider, K. Saeed and N. Ali, *J. Chem. Soc. Pak.*, **30**, 246 (2008).
7. H. Shaikh, N. Memon, H. Khan, M. I. Bhanger and S. M. Nizamani, *J. Chromatogr. A*, **1247**, 125 (2012).
8. M. A. Rauf and S. S. Ashraf, *J. Hazard. Mater.*, **166**, 6 (2009).
9. V. R. Posa, V. Annavaram, J. R. Koduru, V. R. Ammireddy and A. R. Somala, *Korean J. Chem. Eng.*, **33**, 456 (2016).
10. U. G. Akpan and B. H. Hameed, *J. Hazard. Mater.*, **170**, 520 (2009).
11. A. Buthiyappan, A. R. A. Aziz and W. M. A. W. Daud, *Rev. Chem. Eng.*, **32**, 1 (2016).
12. K. Saeed, G. Ali, I. Khan and H. Khan, *J. Chem. Eng. Chem. Res.*, **2**, 671 (2015).

13. S. Valizadeh, M. H. Rasoulifard and M. S. S. Dorraji, *Korean J. Chem. Eng.*, **33**, 481 (2016).
14. A. Nezamzadeh-Ejhieh and Z. Banan, *Desalination*, **284**, 157 (2012).
15. A. Nezamzadeh-Ejhieh and M. Karimi-Shamsabadi, *Appl. Catal. A: Gen.*, **477**, 83 (2014).
16. Z. Shams-Ghahfarokhi and A. Nezamzadeh-Ejhieh, *Mater. Sci. Semiconduct. Process.*, **39**, 265, (2015).
17. A. Nezamzadeh-Ejhieh and N. Moazzeni, *J. Ind. Eng. Chem.*, **19**, 1433 (2013).
18. A. Nezamzadeh-Ejhieh and H. Zabihi-Mobarakeh, *J. Ind. Eng. Chem.*, **20**, 1421 (2014).
19. A. Nezamzadeh-Ejhieh and Z. Banan, *Iran. J. Catal.*, **2**, 79 (2012).
20. A. B. Ghomi and V. Ashayeri, *Iran. J. Catal.*, **2**, 135 (2012).
21. A. Akbarzadeh, M. Samiei and S. Davaran, *Nanoscale Res. Lett.*, **7**, 144 (2012).
22. A. Nezamzadeh-Ejhieh and S. Tavakoli-Ghinani, *Comptes Rendus Chim.*, **17**, 49 (2014).
23. F. Tourinho, R. Franck, R. Massart and R. Perzynski, *Prog. Colloid Polym. Sci.*, **79**, 128 (1989).
24. M. Arain, A. Nafady, Sirajuddin, Z. H. Ibupoto, S. T. H. Sherazi, T. Shaikh, H. Khan, A. Alsalme, A. Niaz and M. Willander, *RSC Adv.*, **6**, 39001 (2016).
25. Y. Zeroual, B. S. Kim, C. S. Kim, M. Blaghen and K. M. Lee, *Appl. Biochem. Biotechnol.*, **134**, 51 (2006).
26. L. You, Z. Wu, T. Kim and K. Lee, *J. Colloid Interface Sci.*, **300**, 526 (2006).
27. S. Haider, N. Bukhari, S. Y. Park, Y. Iqbal and W. A. Al-Masry, *Chem. Eng. Res. Design*, **89**, 23 (2011).
28. A.I. Onen, O. N. Maitera, J. Joseph and E. E. Ebenso, *Int. J. Electrochem. Sci.*, **6**, 2884 (2011).
29. M. S. Mashkour, *Iraqi Natl. J. Chem.*, **46**, 189 (2012).
30. L. N. Dlamini, R. W. Krause, G. U. Kulkarni and S. H. Durbach, *Appl. Water Sci.*, **1**, 19 (2011).
31. N. Bouanimba, R. Zouaghi, N. Laid and T. Sehili, *Desalination*, **275**, 224 (2011).
32. S. A. Djepang, S. Laminsi, E. Njoyim-Tamungang, C. Ngnintedem and J.-L. Brisset, *Chem. Mater. Eng.*, **2**, 14 (2014).
33. J. Z. Liu, T. L. Wang and L. N. Ji, *J. Mol. Catal. B: Enzym.*, **41**, 81 (2006).
34. I. A. Salem, *Appl. Catal. B: Environ.*, **28**, 15 (2000).
35. A. Jayaraman, S. Mas, R. Tauler and A. de Juan, *J. Chromatogr. B*, **910**, 138 (2012).
36. J. Yang, S. Cui, J.-Q. Qiao and H.-Z. Lian, *J. Mol. Catal. A: Chem.*, **395**, 42 (2014).
37. R. Azmat, Z. Khalid, M. Haroon and K. P. Mehar, *Adv. Nat. Sci.*, **6**, 38 (2013).
38. A. Khan, S. Badshah and C. Airoldi, *Chem. Eng. J.*, **171**, 159 (2011).
39. A. Khan, S. Badshah and C. Airoldi, *Polym. Bull.*, **72**, 353 (2015).
40. A. Khan, F. Wahid, N. Ali, S. Badshah and C. Airoldi, *Desalin. Water Treat.*, **56**, 1099 (2015).